

Biochemical Characterization of Recombinant Enterovirus 71 3C Protease with Fluorogenic Model Peptide Substrates and Development of a Biochemical Assay

Luqing Shang,^{a,b} Shumei Zhang,^{a,b} Xi Yang,^{a,b} Jixue Sun,^a Linfeng Li,^{a,b} Zhengjie Cui,^{a,b} Qiuhe He,^c Yu Guo,^a Yuna Sun,^d Zheng Yin^{a,b}

College of Pharmacy & State Key Laboratory of Elemento-Organic Chemistry, Nankai University, Tianjin, People's Republic of China^a; Collaborative Innovation Center of Chemical Science and Engineering (Tianjin), Tianjin, People's Republic of China^b; High-Throughput Molecular Drug Discovery Center, Tianjin International Joint Academy of Biotechnology & Medicine, Tianjin, People's Republic of China^c; National Laboratory of Macromolecules, Institute of Biophysics, Chinese Academy of Science, Beijing, People's Republic of China^d

Enterovirus 71 (EV71), a primary pathogen of hand, foot, and mouth disease (HFMD), affects primarily infants and children. Currently, there are no effective drugs against HFMD. EV71 3C protease performs multiple tasks in the viral replication, which makes it an ideal antiviral target. We synthesized a small set of fluorogenic model peptides derived from cleavage sites of EV71 polyprotein and examined their efficiencies of cleavage by EV71 3C protease. The novel peptide P08 [(2-(*N*-methylamino)benzoyl) (NMA)-IEALFQGPPK(DNP)FR] was determined to be the most efficiently cleaved by EV71 3C protease, with a kinetic constant k_{cat}/K_m of $11.8 \pm 0.82 \text{ mM}^{-1} \text{ min}^{-1}$. Compared with literature reports, P08 gave significant improvement in the signal/background ratio, which makes it an attractive substrate for assay development. A Molecular dynamics simulation study elaborated the interactions between substrate P08 and EV71 3C protease. Arg39, which is located at the bottom of the S2 pocket of EV71 3C protease, may participate in the proteolysis process of substrates. With an aim to evaluate EV71 3C protease inhibitors, a reliable and robust biochemical assay with a Z' factor of 0.87 ± 0.05 was developed. A novel compound (compound 3) (50% inhibitory concentration [IC_{50}] = $1.89 \pm 0.25 \text{ }\mu\text{M}$) was discovered using this assay, which effectively suppressed the proliferation of EV 71 (strain Fuyang) in rhabdomyosarcoma (RD) cells with a highly selective index (50% effective concentration [EC_{50}] = $4.54 \pm 0.51 \text{ }\mu\text{M}$; 50% cytotoxic concentration [CC_{50}] > $100 \text{ }\mu\text{M}$). This fast and efficient assay for lead discovery and optimization provides an ideal platform for anti-EV71 drug development targeting 3C protease.

Enterovirus 71 (EV71) is the causative agent of hand, foot, and mouth disease (HFMD), which typically affects infants and children (1). HFMD usually presents as a mild febrile disease with a localized rash, but some patients may develop infection of the central nervous system (CNS) with illness ranging from aseptic meningitis through fatal encephalitis (2). In the last decade, outbreaks of HFMD have regularly reoccurred through Asia (3, 4). According to data from the Chinese Center for Disease Control and Prevention (CDC), more than 420,000 cases of HFMD, with 70 deaths, were reported in China in April 2014. Currently, there is no antiviral therapy available for treatment of HFMD.

EV71 belongs to the genus *Enterovirus* in the family *Picornaviridae* (5–7). Similar to other picornaviruses, EV71 contains a single-stranded, positive-sense RNA encoding a large polyprotein precursor (8, 9). The polyprotein is further cleaved into four structural proteins (VP1 to VP4) to form the viral capsid and seven nonstructural proteins (2A to 3D) for virus replication via the 2A protease and 3C protease (10, 11). Except for the cleavage of VP1/2A by the 2A protease (12) and the RNA-dependent cleavage of VP2/4 (13), the 3C protease is absolutely required for the cleavage of other junction sites within the polyprotein (14–16). Meanwhile, EV71 3C reportedly interferes with the polyadenylation of host cell RNA by digesting CstF-64, a critical host factor for 3' pre-mRNA processing, suggesting a novel mechanism by which picornaviruses utilize 3C^{pro} to impair host cell function (17). In addition, the 3C protease can also cleave numerous factors and regulators associated with cellular DNA-dependent RNA polymerases I, II, and III, such as the octamer-binding protein (OCT-

1), TATA box-binding protein (TBP), cyclic AMP-responsive element-binding protein (CREB), transcription activator p53, histone H3, and DNA polymerase III (18–21). The pivotal role of 3C protease in EV71 replication makes it an attractive target for antiviral discovery (22).

The crystal structure of unliganded EV71 3C protease showed that EV71 3C protease folded into two domains that are related to other picornaviral 3C protease structures (23). The complex structures of EV71 mutants H133G, E71A, E71D with the inhibitor rupintrivir are similar to that of the unliganded protease structure (24). Lu et al. thoroughly characterized the 3C proteases from EV71 and CVA16 and reported a series of structures of both enzymes in free, peptide-bound, or inhibitor-bound form (25). These findings provided precise molecular insights into the substrate recognition and inhibition of 3C protease.

Received 3 November 2014 Returned for modification 5 November 2014
Accepted 17 November 2014

Accepted manuscript posted online 24 November 2014

Citation Shang L, Zhang S, Yang X, Sun J, Li L, Cui Z, He Q, Guo Y, Sun Y, Yin Z. 2015. Biochemical characterization of recombinant enterovirus 71 3C protease with fluorogenic model peptide substrates and development of a biochemical assay. *Antimicrob Agents Chemother* 59:1827–1836. doi:10.1128/AAC.04698-14.

Address correspondence to Yuna Sun, sunyn@moon.ibp.ac.cn, or Zheng Yin, zheng_yin@nankai.edu.cn.

Copyright © 2015, American Society for Microbiology. All Rights Reserved.
doi:10.1128/AAC.04698-14

Profiling of the EV71 3C protease substrate could not only provide in-depth knowledge of catalytic mechanism at a molecular level, which would facilitate the design of potent protease inhibitors, but also lead to development of a reliable and robust biochemical assay for screening. In 2008, Kuo et al. synthesized six dodecapeptide substrates derived from the EV71 protease cleavage site and one dodecapeptide substrate (TSAVLQSGFRKM) from the severe acute respiratory syndrome coronavirus (SARS-CoV) protease autoprocessing site for biochemical characterization of the EV71 3C protease by determining their specificities using high-performance liquid chromatography (HPLC). The results showed that EV71 3C protease cleaved TSAVLQSGFRKM more efficiently than the other six substrates (26). Eight peptides derived from CVA16 polyprotein and three peptides derived from EV71 polyprotein were also investigated for their susceptibilities to 3C cleavage via HPLC assay, and the peptide (IGNTIEALFQGPPKER) corresponding to 2C-3A junction site of CVA16 could be efficiently processed by both proteases ($V = 8.37 \mu\text{M}/\text{min}$ for EV71 and $10.72 \mu\text{M}/\text{min}$ for CVA16) (25). However, the HPLC assay is limited to conveniently determine the substrate specification, and the technique of fluorescence resonance energy transfer (FRET) is commonly used for the preparation of fluorogenic substrates for biochemical characterization of proteases and protease inhibitor screening (27). A fluorogenic peptide, *p*-(*p*-dimethylaminophenylazo)benzoic acid (Dabcyl)-KTSAVLQSGFRKME-5-[(2-aminoethyl)amino]naphthalene-1-sulfonic acid (Edans) ($K_m = 5.8 \mu\text{M}$; $k_{\text{cat}} = 0.45 \text{ min}^{-1}$) was synthesized for the EV71 3C protease inhibitor screening (26). Cui et al. (23) also examined three fluorogenic substrates corresponding to the EV71 polyprotein autoprocessing site 3B-3C, the internal cleavage site (amino acids [aa] 251/252 with the Q-G junction) of CstF-64, and the SARS-CoV autoprocessing site. Contrary to the results of Kuo et al., Dabcyl-TSAVLQSGFRKM-Edans, corresponding to the autoprocessing site of SARS-CoV protease, was demonstrated to be an unfavorable substrate for EV71 3C protease (the K_m and V_{max} could not be precisely determined by Michaelis-Menten equation fitting because of its poor enzyme activity). In their hands, though the peptide substrate Dabcyl-RTATVQGPSLDFKE-Edans, corresponding to the EV71 3B-3C junction, displayed the best EV71 3C protease proteolytic activity, it still had a low cleavage rate and exhibited a low kinetic constant k_{cat}/K_m of $7.1 \times 10^{-4} \mu\text{M}^{-1} \text{ min}^{-1}$ (23), indicating that the peptide Dabcyl-RTATVQGPSLDFKE-Edans may not be the optimal substrate for EV71 protease inhibitor screening.

The aim of this study was to biochemically characterize EV71 3C protease with an aim to develop a reliable and efficient assay for the screening of EV71 3C protease inhibitors. The substrate specificity was defined using a series of fluorogenic peptides mapped from the cleavage sites on the EV71 polyprotein. A peptide [P08, NMA-IEALFQGPPE(DNP)FR] with FRET groups corresponding to the cleavage site of the 2C-3A junction was determined to be the most efficiently cleaved by EV71 3C protease, with a kinetic constant k_{cat}/K_m of $11.8 \pm 0.82 \text{ mM}^{-1} \text{ min}^{-1}$. Compared with the substrates reported previously, P08 gave the highest signal-to-background ratio, which makes it an ideal substrate for assay development. The impacts of pH, temperature, and dimethyl sulfoxide (DMSO) concentration were systematically studied. With a goal to evaluate EV71 3C protease inhibitors, a reliable and robust biochemical assay with a Z' factor of 0.87 ± 0.05 was developed. This fast and efficient assay for lead discovery and optimization

provides an ideal platform for anti-EV71 drug development targeting 3C protease.

MATERIALS AND METHODS

Expression and purification of the EV71 3C protease. The cDNA encoding the EV71 3C protease (aa 1 to 183) was amplified by reverse transcription-PCR (RT-PCR) using the genomic RNA of EV71 (EV71 isolate BJ/CHN/2008; GenBank accession no. [ADT71698.1](http://www.ncbi.nlm.nih.gov/nuccore/ADT71698.1)) as the template and cloned into the NdeI and NotI sites of the pET28a expression vector (GE Healthcare) (28–30). The plasmid was transformed into *Escherichia coli* strain BL21(DE3), and transformed cells were cultured at 37°C in LB medium containing 100 mg/liter kanamycin. Protein expression was induced with 0.5 mM isopropyl- β -D-1-thiogalactopyranoside for 14 h after the optical density at 600 nm (OD_{600}) of the culture reached 0.6. Cells harvested by centrifugation were resuspended in lysis buffer (50 mM Tris-HCl [pH 7.0], 150 mM NaCl, 10% glycerol) and then homogenized with a ultra-high-pressure cell disrupter (JNBIO, Guangzhou, China) at 4°C. The lysate was clarified by centrifugation at $20,000 \times g$ for 30 min at 4°C. The supernatant was loaded onto a 15-ml Ni-nitrilotriacetic acid (NTA) column equilibrated in lysis buffer. The nonspecific contaminants were then removed by washing with 20 column volumes of lysis buffer. The 3C protease was subsequently eluted with 200 mM imidazole in lysis buffer. The eluate was further purified with a Superdex 200 gel filtration column (GE Healthcare). The purified 3C protease was then concentrated to approximately 10 to 12 mg/ml in a buffer containing 20 mM Tris-HCl (pH 7.0), 150 mM NaCl, 1 mM EDTA, 5 mM dithiothreitol [DTT], and 10% glycerol.

Synthesis of substrate peptides. A fluorogenic peptide library, P01 to P17, has been developed by solid-phase peptide synthesis using standard Fmoc [N-(9-fluorenyl) methoxycarbonyl] techniques (31). The cleavage of the peptide from 2-chlorotriethyl chloride resin and removal of all of the side chain protecting groups were achieved in trifluoroacetic acid solution. Peptides were purified by semipreparative HPLC (Waters, USA) using a Waters 515 device equipped with a 2489 dual-absorbance detector and analyzed on an Thermo C₁₈ 100-Å, 5- μm , 250- by 10-mm column (unless otherwise specified) using gradients of CH₃CN (0.1% trifluoroacetic [TFA])-H₂O (0.1% TFA) as the elution system with a flow rate of 1 ml/min. Here, 5-[(2-aminoethyl)amino]naphthalene-1-sulfonic acid (Edans) and 2-(*N*-methylamino)benzoyl (NMA) are the fluorescent donor moieties; *p*-(*p*-dimethylaminophenylazo)benzoic acid (Dabcyl) and 2,4-dinitrophenyl (DNP) are the quencher moieties. Peptide homogeneity and identity were analyzed by analytical HPLC (Dionex, China) and liquid chromatography-mass spectrometry (LC-MS) (Shimadzu, Japan), respectively.

In vitro cleavage assay. For each fluorogenic peptide substrate, the cleavage activity of purified EV71 3C protease was determined in a reaction volume of 100 μl , using 10 μl enzyme (50 μM) and 10 μl peptides (maximum concentration, 5 mM) in the reaction buffer (50 mM Tris [pH 7.0], 150 mM NaCl, 1 mM EDTA, 2 mM DTT, 10% glycerol) to yield a final concentration of 5 μM enzyme and substrate peptide at concentrations ranging from 5 μM to 500 μM . Cleavage assay mixtures were incubated in a 96-well flat-bottom black microplate at 30°C for 2 h, and then reactions were terminated by the addition of equal volume of acetonitrile. Once the protease cleaved the peptide bond, resulting in separation of the fluorophore and fluorescence quencher moiety, the fluorescence of the fluorophore was recovered by disappearance of the FRET effect in proportion to the degree of the protease reaction. The relative fluorescence of the reactive mixture was measured every 10 s over a period of 2 h on a Tecan Safire2 (Switzerland) multimode microplate reader (excitation wavelength [λ_{ex}] = 340 nm and emission wavelength [λ_{em}] = 490 nm for Edans/Dabcyl; λ_{ex} = 340 nm and λ_{em} = 440 nm for NMA/DNP). The ratio of the final fluorescence signal of the mixture to the background of the substrate (S/B) was calculated to quickly characterize the cleavage efficiencies of substrates, which are classically defined as $S/B = \text{mean signal}/\text{mean background}$ (32).

To determine the velocities of product formation, the instrument was precalibrated with the free fluorescent moiety Edans or NMA standard to calculate the relationship between relative fluorescence unit and substrate concentration. The initial velocities were calculated for all of the cleavage products from three independent experiments. The kinetic parameters K_m , V_{max} , and catalytic efficiency (k_{cat}/K_m) were calculated assuming Michaelis-Menten kinetics for all of the cleavage peptides. No significant hydrolysis of the peptide substrates was observed in the absence of EV71 3C protease.

In order to determine the optimal reaction conditions for 3C protease, various salt concentrations, pH values, temperatures, and dimethyl sulfoxide (DMSO) concentrations were used. The protease and substrate were incubated at different combinations of NaCl concentration and pH. The pH values selected for the protease proteolysis were 5, 6, 7, and 8, and each pH was carried out with different NaCl concentrations (100, 150, 200, and 500 mM). To determine the temperature condition, the protease reaction sample was incubated at different temperatures (10, 20, 30, 40, and 50°C). The effect of DMSO on enzymatic activity of the EV71 3C protease was determined by assays in buffer containing DMSO concentrations varying from 0.5% to 10% (vol/vol). Fluorescence was measured following incubation at 30°C for 2 h. All reactions were performed in triplicate to determine the effects of salt concentration, pH, temperature, and DMSO on protease enzymatic activity.

MD simulation. To run molecular dynamics (MD) simulations, enzyme-substrate complexes were first prepared. The receptor enzyme (PDB 4GHQ) was obtained from the Protein Data Bank (29). The ligand peptides were positioned in the protein similar to the position in the work by Lu et al. (25), which solved the crystal structure of the CVA16 3C protease with the peptide FAGLRQAVTQ (PDB 3SJ9). We aligned the structure of 4GHQ, maintained the coordinates of the backbone and β -carbon of 3SJ9's ligand, and replaced the residues to substitute for our ligand substrates. The Leap module of Amber12 with the standard Amber99SSB force field was then used to build the enzyme-substrate complexes. The side chains of ligand peptides are added automatically in Leap. The existence of the β -carbon ensures the correct direction of side chains (33). Chloride ions were added as counterions to neutralize the complexes (34). TIP3PBOX (35) was used to add an explicit water box, and the distance between the edges of the box and the closet atoms of the complexes was set to 10 Å.

There are two steps in the minimization procedure to eliminate bad contacts. Every step was using steepest-descent minimization, followed by conjugate gradient minimization with the same steps. First, with the complex fixed, solvent and ions were subjected to a 2,000-step optimization (1,000 steps of steepest-descent minimization and 1,000 steps of conjugate gradient minimization). Second, the whole system was optimized using 5,000 steps of minimization. After the minimization procedure, every solvated complex was equilibrated by 60 ps of heating from 0 K to 300 K and 60 ps of density equilibration. Both simulations were run with a 2-fs time step, $10\text{-kcal} \cdot \text{mol}^{-1} \cdot \text{\AA}^{-2}$ constraints on the complex, and Langevin dynamics (36) for temperature control. Before molecular dynamics simulation, an additional 1-ns equilibration was run to refine the interactions of receptor and ligand. In the first 0.5 ns, the distances of all the hydrogen bonds between residues of receptor and all the main chains of ligand and the side chain of the second peptide from the C terminus were restrained. In the remaining 0.5 ns, a $2\text{-kcal} \cdot \text{mol}^{-1} \cdot \text{\AA}^{-2}$ constraint was set on the complex to avoid a significant structure change. Then, the final phase of equilibration of every system was used to run a 3-ns molecular dynamics simulation. The conditions were the same as for the equilibration procedure but without restraints or constraints. The SHAKE algorithm (44) was applied to keep all bonds involving hydrogen atoms rigid.

Z' factor calculation. The most efficient substrate, NMA-IEALFQGP PK(DNP)FR (20 μM final concentration), was added to 96-well flat bottom black microplates containing EV71 3C protease at a 1 μM final concentration (positive control) or buffer without protease (negative

control). Since the Z' factor is dependent on means and standard deviations (SD), each combination had 60 wells. The plate was incubated at 30°C for 2 h, and fluorescence readings were obtained. The Z' factor is calculated from the means and SD of fluorescence from positive (in the presence of protease) and negative (in the absence of protease) control plates as previously described (32): $Z' \text{ factor} = 1 - [(3\sigma_s + 3\sigma_c)/(\mu_s - \mu_c)]$, where σ_s and σ_c are the standard deviations for the positive and negative controls, respectively, and μ_s and μ_c are the means for the positive and negative controls, respectively.

Enzyme inhibition assay. In the *in vitro* cleavage assay, the peptide NMA-IEALFQGPCK(DNP)FR was demonstrated to be most efficiently processed by EV71 3C protease, which was used as the substrate for the enzyme inhibition assay. Here, three tested compounds (see Table 3) were synthesized as described previously (26). The assays were performed with 100- μl samples containing 1 μM protease, 20 μM substrate, and various concentrations (10 μM to 0.156 μM) of the tested compounds in a buffer of 50 mM Tris, pH 7.0. To determine the inhibitory effects of the various compounds, the compound and the enzyme were preincubated at 30°C for 30 min prior to addition of the substrate. The reaction mixture was then incubated for 2 h at 30°C. The reaction was terminated by the addition of acetonitrile. The initial velocities of the enzymatic reactions were determined and fitted to a sigmoidal dose-response equation with non-linear regression analysis using the program GraphPad Prism. The data from three independent assays were used as input for Prism to determine 50% inhibitory concentrations (IC_{50}s).

Viruses and cells. Human rhabdomyosarcoma (RD) cells were grown in Dulbecco's modified Eagle's medium (DMEM) (GIBCO) supplemented with 10% fetal bovine serum (FBS) (GIBCO) at 37°C in a 5% CO_2 humidified incubator.

The EV71 reporter virus system [EV71(FY)-Luc pseudotype virus system] containing pcDNA6-FY-capsid and pEV71-Luc-replicon lacking the P1 region were kindly supplied by Wenhui Li, National Institute of Biological Sciences, Beijing, China.

Antiviral assay. The EV71 pseudotype virus [EV71(FY)-Luc] was produced by using a method developed as previously described (11, 37). Briefly, the pEV71-Luc subgenomic replicon was linearized through digestion with SalI restriction enzyme and was used as a template for RNA transcription. The EV71 replicon RNA transcripts were prepared *in vitro* by using Ambion MEGAscript kits. The pcDNA6-FY-capsid plasmid was transfected into HEK-293T cells at 60 to 80% confluence. After 24 h post-transfection, EV71 subgenomic replicon RNA was then transfected using Lipofectamine 2000 (Invitrogen). EV71 pseudotype virus was harvested at 24 h after RNA transfection with two freeze-thaw cycles. To quantify the EV71 pseudotype virus, the stocks were serially diluted 10-fold and incubated with RD cells for 24 h at 37°C. The cells were then harvested, and the luminescence was detected as described in the manufacturer's protocol for the Bright-Glo luciferase assay system (Promega).

Fifty percent effective concentrations (EC_{50}s) of tested compounds were determined on RD cells. RD cells (3×10^4 per well in 100 μl 10% FBS-DMEM) were seeded in 96-well plates and cultured at 37°C and 5% CO_2 overnight. Cells were treated with a dilution gradient of different compounds, ranging from 0.39 to 100 μM . EV71(FY)-Luc virus at a multiplicity of infection (MOI) of 1 was added to 96-well plates. The luminescence was measured at 490 nm after 24 h postinfection, and EC_{50}s of compounds were calculated using log (concentration) versus luminescence (490 nm) in GraphPad Prism.

Cytotoxicity. The cytotoxicity was measured by WST-1 cell proliferation using a cytotoxicity assay kit according to the manufacturer's protocol (catalog no. 05015944001; Roche, USA). Briefly, RD cells (3×10^4 per well in 100 μl 10% FBS-DMEM) were cultured at 37°C under 5% CO_2 in 96-well plates, followed by the addition of 50 μl compound solution with a concentration ranging from 0.78 to 200 μM . The cells were incubated at 37°C for 24 h, and then 10 μl WST-1 reagent was added to each well. The luminescent signals were read at 490 nm with a microplate reader (Bio-Rad, USA). The percentage of viable cells after treatment with

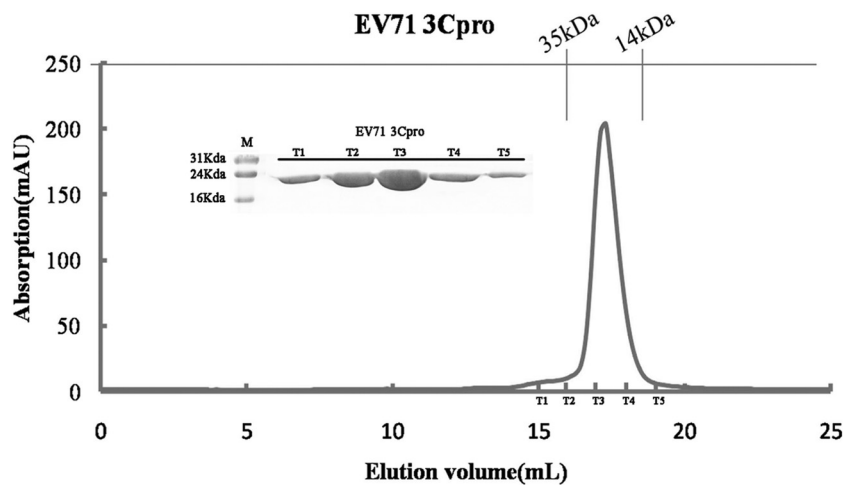


FIG 1 Size exclusion chromatography (SEC) of EV71 3C protease. The EV71 3C protease was purified by HPLC with a retention volume of 17 ml, and samples (T1 to T5) obtained during the purification process were analyzed by SDS-PAGE and staining with Coomassie brilliant blue R-250.

different concentrations of compound was calculated as follows: percentage of inhibition = $100 \times \text{OD}_{490}$ of treated sample/ OD_{490} of cell control sample. The 50% cytotoxic concentration (CC_{50}) was defined as the concentration of compound that reduced the treated RD cells by 50% relative to the untreated control cells and was calculated using GraphPad Prism.

RESULTS

Expression and purification of EV71 3C protease. EV71 3C protease was expressed and purified as described previously (29). No amino acid substitutions were introduced in the recombinant protease sequence. After the first induction at 37°C, the majority of 3C-like protease was found in the fraction of the cell lysate. The lysate was induced with isopropyl-β-D-1-thiogalactopyranoside for an additional 14 h. As a result, most of the EV71 3C protease was found in the soluble fraction. The protease was purified by HPLC with a retention volume of 17 ml, and SDS-PAGE analysis revealed the presence of a major protein with molecular mass of 22 kDa, which indicates that recombinant EV71 3C protease was obtained with over 95% purity (Fig. 1).

Substrate specificity of EV71 protease. The cleavage activity of the EV71 3C protease was assayed by fluorescence release from a set of synthesized fluorogenic peptide substrates (Table 1) derived from the junctions of polyprotein (TW/2231/98) that were cleaved by 3C protease (26). The ratios of signal to background were used to quickly evaluate the cleavage efficiency of EV71 3C

protease against the peptide substrates. Two reported substrates with FRET pair Dabcyl/Edans, P01 (Dabcyl-RTATVQGPSLDFK E-Edans) (23) and P02 (Dabcyl-TSAVLQSGFRKME-Edans) (26), were prepared as the controls. The signal-to-background (S/B) ratios for P01 and P02 were 5.7 and 2.2, respectively, which indicated that the reported substrate P01 could be more efficiently cleaved by EV71 3C protease than P02. A shorter-wavelength FRET pair, NMA/DNP, was chosen for our study to improve the signal-to-background ratio (38). The FRET peptides P03 (NMA-RTATVQGPSLDFK-DNP) and P04 [NMA-TSAVLQSGFRK(DN P)M], which linked the NMA group and the quencher group DNP to the ε-amino function of Lys, were obtained to test *in vitro* cleavage activity against EV71 protease compared with the reported substrates. A slightly improved S/B ratio was observed for the peptide P03 (S/B, 6.5) compared to the corresponding peptide P01 (S/B, 5.7). A similar result was observed in the comparison of substrate P04 (S/B, 2.8) and the corresponding substrate P02 (S/B, 2.2). Based on this result, the peptides corresponding to the cleavage sites of EV71 3C protease with the NMA/DNP pair (P05 to P09) were synthesized and evaluated for their specificity (Table 1).

Though these peptides had the same Gln-Gly pair interaction at the P1-P1' position, the proteolysis efficiencies of the initial set of peptides (P05 to P09) in the cleavage assay varied significantly (S/B, 1.8 to 15.3) (Fig. 2A). Among all substrates, the highest

TABLE 1 Synthesized peptides derived from the polyprotein of EV71

Peptide	Sequence	Cleavage site	S/B	Mutational peptides		
				Peptide	Sequence	S/B
P01	Dabcyl-RTATVQGPSLDFKE-Edans	3B-3C	5.7	P11	NMA-IAALFQGPPK(DNP)FR	4.6
P02	Dabcyl-TSAVLQSGFRKM-Edans	SARS-CoV	2.2	P12	NMA-IELLFQGPPK(DNP)FR	8.2
P03	NMA-RTATVQGPSLDFK(DNP)	3B-3C	6.5	P13	NMA-IEAALFQGPPK(DNP)FR	9.7
P04	NMA-TSAVLQSGFRK(DNP)M	SARS-CoV	2.8	P14	NMA-IEALAQGPPK(DNP)FR	1.9
P05	NMA-RQAVTQGFPTELK-DNP	VP2-VP3	7.7	P15	NMA-IEALFQSPPK(DNP)FR	1.9
P06	NMA-QTGTIQGDRVADK-DNP	VP3-VP1	1.8	P16	NMA-IEELFQGPPK(DNP)FR	2.0
P07	NMA-DEAMEQGVSDYIK-DNP	2A-2B	3.6	P17	NMA-IEALKQGPPK(DNP)FR	1.9
P08	NMA-IEALFQGPPK(DNP)FR	2C-3A	15.3			
P09	NMA-LFAGFQGAYSGAK-DNP	3A-3B	1.8			
P10	Dabcyl-IEALFQGPPKERE-Edans	2C-3A	6.8			

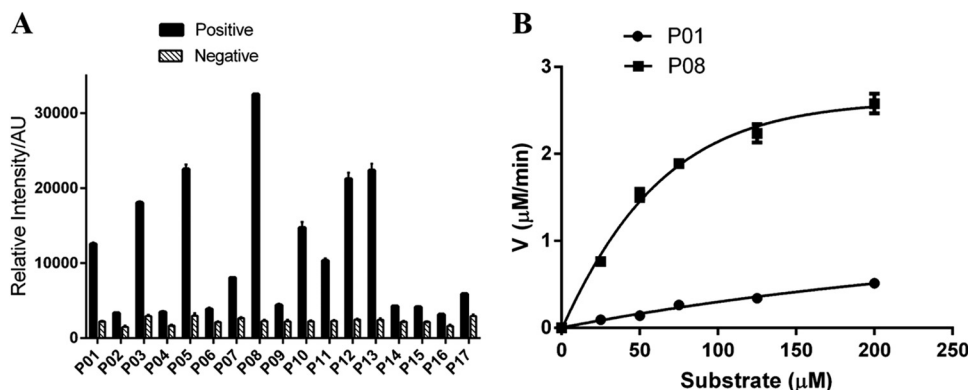


FIG 2 (A) *In vitro* cleavage activity of EV71 protease with different peptide substrates. Positive, relative fluorescence intensity of each substrate (50 μ M) incubated with EV71 3C protease (5 μ M); negative, background of each peptide. (B) Substrate specificity of EV71 3C protease. The proteolytic reactions were performed using substrates P01 and P08. ●, control substrate P01 derived from the 3B-3C junction; ■, novel substrate P08 derived from the 2C-3A junction. The data presented are mean values from experiments in triplicate, and the error bars represent the standard deviations.

cleavage efficiency was observed for the substrate peptide P08 [NMA-IEALFQGPPK(DNP)FR] (S/B, 15.3), which represents the native EV71 protease cleavage sites at the 2C-3A junction. Moderate proteolytic efficiency was observed for peptide P05 (S/B, 7.7), which corresponds to VP2-VP3. The substrate P07 showed much lower cleavage efficiency, with an S/B value of 3.6, which corresponds to the 2A-2B junction. Poor enzymatic activity was observed against the substrate peptides P06 and P09 (S/B, 1.8), representing the VP1-VP3 and 3A-3B junction sites, respectively.

As the substrate P08 exhibited the highest cleavage efficiency, peptide P10, with the same sequence as P08 but with the FRET pair Dabcyl/Edans, was also prepared to study the impact of the FRET pair. P10 was only moderately hydrolyzed by 3C protease (S/B, 6.8), with cleavage being less efficient than that of P08 (S/B, 15.3).

To further elucidate the substrate specificities of the 3C proteases, seven site-directed peptide variants, P11 to P17, with substitutions of amino acids in the P5 to P1' region of P08 were examined (Fig. 2A). Peptide P11, with a P5 site variant E to A within the context of the P08 sequence, showed a relatively lower activity (S/B, 4.6). Peptides P12 and P13, with a P4 site variant A to L and P3 site variant L to A, respectively, represented moderate cleavage efficiency (S/B, 8.2 and 9.7), whereas peptide P16, with the variant A to F at the P4 position, exhibited poor cleavage efficiency (S/B, 2.0). Moreover, it is notable that EV71 3C protease showed strong preference for the P2 and P1' residues. Variants at the P2 and P1' positions dramatically reduced the cleavage efficiency by EV71 protease, as observed by substrates P14, P15, and P17, with the S/B values of less than 2.

Optimization of cleavage assay conditions. Peptide P08, with the highest signal-to-background ratio, was selected as the substrate for optimization of cleavage assay conditions. The effect of pH on the enzymatic activity of EV71 3C protease was determined by assays using buffers in the pH range from 5 to 8 (Fig. 3A). In agreement with earlier reports on EV71 3C protease (23), the pH optimum for reaction for the peptide substrate was 7.0. It is noteworthy that the protease almost lost the enzymatic activity when the pH was decreased to 5. Changes in salt concentration from 100 mM to 500 mM NaCl produced little effect on the enzymatic activity. The combination of salt concentration and pH value that gave the highest proteolytic activity was 150 mM NaCl and pH 7.0.

These reaction conditions were then applied throughout the downstream assay development.

The effects of the temperature on proteolysis are shown in Fig. 3B. The maximum fluorescence was observed within 2 h of incubation at 30°C, while the protease activity decreased with increasing or decreasing temperature beyond 30°C. Hence, the optimal temperature for protease activity is considered 30°C.

The effect of DMSO on the proteolytic activity of EV71 3C protease was also determined (Fig. 3C). No significant difference in protease cleavage efficiency was observed with DMSO concentrations of 0.5% to 10% (vol/vol), indicating that this assay is not affected by up to 10% DMSO.

Kinetic analysis of EV71 3C protease substrates. The kinetic parameters for proteolysis of substrates were determined in order to quantify the cleavage efficiency and substrate specificity of EV71 3C protease (Table 2). For the control substrates, the K_m and k_{cat} values of P01 were determined to be 82.5 μ M and 0.12 min^{-1} , respectively, while for the substrate P02, the K_m and k_{cat} could not be precisely determined because of its low activity. Of all 13 peptides, the kinetic parameters for most of the substrates could be calculated assuming Michaelis-Menten kinetics, except for P06, P09, P14, P15, P16, and P17, which had low S/B values (no more than 2). The substrate P08 [NMA-IEALFQGPPK(DNP)FR] had the lowest K_m (43.1 ± 2.3 μ M) and the highest turnover number (0.51 ± 0.12 min^{-1}) of all the peptide substrates, resulting in the highest k_{cat}/K_m (11.8 ± 0.82 $\mu\text{M}^{-1} \text{min}^{-1}$). This clearly demonstrated that P08 was the most suitable substrate for EV71 3C protease cleavage. Compared with the control substrate P01 (Fig. 2B), EV71 3C protease displayed much higher enzymatic activity against the substrate P08 due to the cumulative effects of change in both K_m and k_{cat} .

Molecular dynamics. In order to gain in-depth understanding of the catalytic mechanism of EV71 3C protease at the molecular level, molecular dynamics simulations and molecular docking were applied to build structural models of the complexes and further determine the relative contributions of different residues to the overall binding affinity. We docked the P6 to P1' portions (such as RTATVQG for P01 and IEALFQG for P08) of the peptides into the substrate-binding groove of EV71 3C protease for molecular dynamics simulation (Fig. 4A).

EV71 3C protease is a specific protease that preferentially rec-

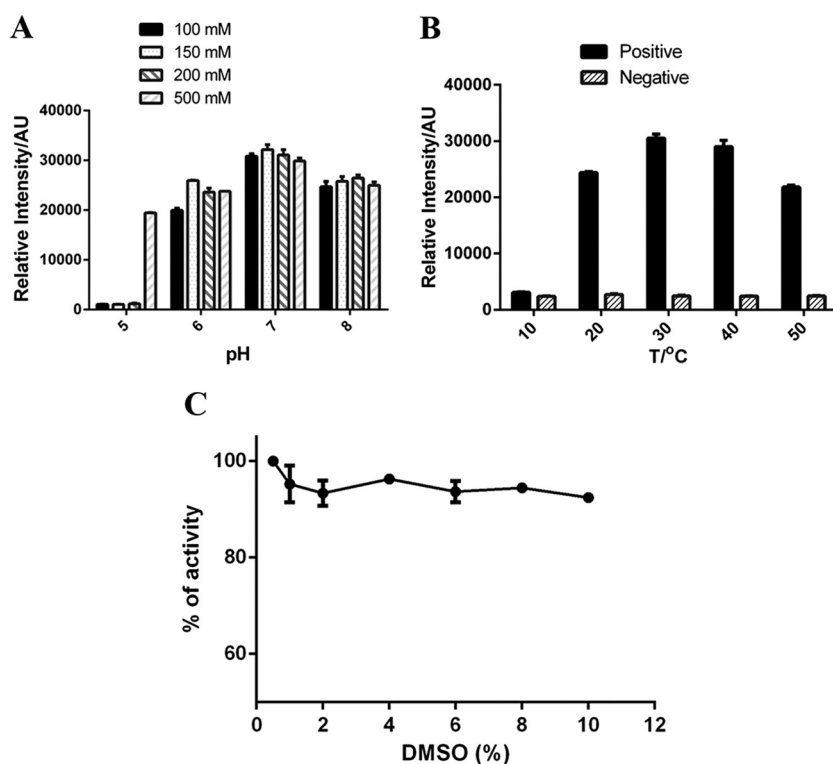


FIG 3 (A) Optimization of salt concentration and pH for protease assay. The fluorescence of proteolytic reactions were measured in different reaction buffers with various combinations of salt (100 to 500 mM) and pH (pH 5 to 8). (B) Effect of temperature (10 to 50°C) on enzymatic activity. Positive, relative fluorescence intensity of substrate after incubation with EV71 3C protease. Negative, background intensity of the substrate. (C) Effect of DMSO on protease activity. Various concentrations (0.5 to 10%) of DMSO were used in the reaction buffer. The data presented are mean values from experiments in triplicate, with the error bars representing the standard deviations.

ognizes substrates with the Q-G junction. In the molecular model, P1'-Gly was oriented toward the S1' subsite constituted by the hydrophobic parts of residues His24, Phe25, His108, Gly145, and Cys147. In the natural cleavage sites within the EV71 polyprotein precursors, the P1 position is invariably occupied by Gln. This residue is accommodated by the His161 and Thr142 at the bottom

of the S1 pocket. The side chain of P1-Gln formed three strong hydrogen bonds (2.5 to 3.0 Å) with these two residues (Fig. 4B).

In contrast to the high conservation of P1-Gln, the hydrophobic S2 pocket is large enough to accommodate various side chains of the substrate. Consistently, the P2 residues of substrates (P03 and P05 to P09) have certain flexibility. The best selectivity is for

TABLE 2 Cleavage efficiencies of fluorogenic peptide substrates^a

Peptide	Sequence	K_m (μ M)	k_{cat} (min^{-1})	k_{cat}/K_m ($\text{mM}^{-1} \text{min}^{-1}$)
P01	Dabcyl-RTATVQGPSLDFKE-Edans	82.5 ± 3.8	0.12 ± 0.01	1.45 ± 0.1
P02	Dabcyl-TSAVLQSGFRKM-Edans	ND	ND	ND
P03	NMA-RTATVQGPSLDFK(DNP)	58.2 ± 4.7	0.21 ± 0.08	3.6 ± 0.72
P04	NMA-TSAVLQSGFRK(DNP)M	75 ± 3.2	0.02 ± 0.008	0.27 ± 0.07
P05	NMA-RQAVTQGFPTELK-DNP	92.4 ± 5.3	0.2 ± 0.02	2.2 ± 0.13
P06	NMA-QTGTIQGDRVADK-DNP	ND	ND	ND
P07	NMA-DEAMEQGVSDYIK-DNP	73.5 ± 6.1	0.03 ± 0.01	0.4 ± 0.11
P08	NMA-IEALFQGPPK(DNP)FR	43.1 ± 2.3	0.51 ± 0.12	11.8 ± 0.82
P09	NMA-LFAGFQGGAYSGAK-DNP	ND	ND	ND
P10	Dabcyl-IEALFQGPPKFR-Edans	63.2 ± 3.6	0.17 ± 0.03	2.69 ± 0.15
P11	NMA-IAALFQGPPK(DNP)FR	75 ± 5.3	0.16 ± 0.03	2.13 ± 0.24
P12	NMA-IELLFQGPPK(DNP)FR	48.2 ± 3.6	0.24 ± 0.06	5 ± 0.38
P13	NMA-IEAALFQGPPK(DNP)FR	66.7 ± 5.3	0.3 ± 0.05	4.5 ± 0.14
P14	NMA-IEALAQGPPK(DNP)FR	ND	ND	ND
P15	NMA-IEALFQSPPK(DNP)FR	ND	ND	ND
P16	NMA-IEELFQGPPK(DNP)FR	ND	ND	ND
P17	NMA-IEALKQGPPK(DNP)FR	ND	ND	ND

^a Data are means and standard deviations from experiments performed in triplicate. ND, not determined due to poor cleavage efficiency.

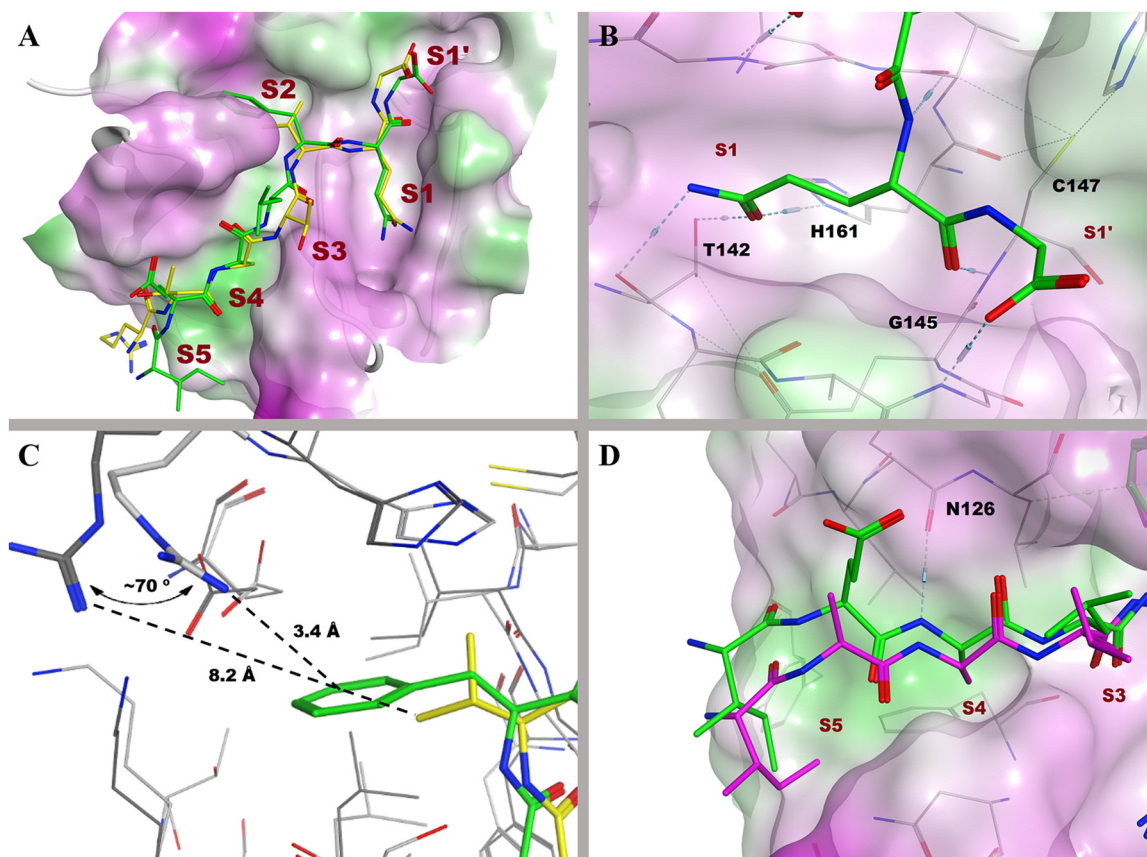


FIG 4 (A). Surface representation of EV71 3C protease complexed with the P6 to P1' portions of P01 (yellow) and P08 (green). (B) Detailed interaction between P1' and P1 of peptide P08 and the EV71 3C protease. Hydrogen bonds are shown as dashed lines. (C) Stick model of EV71 protease interacting with P2 positions of peptide P01 (yellow) and P08 (green). Arg39 represents different rotation in the models. (D) Comparison of the P5 positions of P08 (green) and P11 (magenta).

the relative large hydrophobic residue Phe, as observed with P08, which has the highest cleavage activity. A variant with Phe to Ala or Lys at the P2 position resulted in a dramatic reduction of the cleavage site (P08 versus P14 and P17), indicating the pivotal role of the P2 residue. The Phe side chain mainly hydrophobically contacted with Lys130 and Glu71 at the S2 specificity pocket of the EV71 3C protease. The introduction of the small residue Ala at P2 left most of the specificity pocket unoccupied. Likewise, the introduction of the basic amino acid Lys may not be appropriate for the hydrophobic S2 pocket, as it led to dramatically decreased cleavage efficiency. Interestingly, Arg39, located at the bottom of S2 pocket, provided different orientations depending on the appearance of a benzene ring in the P2 side chain when we stimulated these peptides. In the molecular model of P08, as well as peptide variants P11, P12, and P13, Arg39 strikingly rotated about 70° toward to the Phe residue and interacted with the benzene ring, while no such rotation was observed in other substrates without Phe at the P2 position, such as P01 (Fig. 4C). Consistently, Arg39 has been demonstrated to play a key role in the EV71 protease proteolysis process (24). This should partially account for the observed dramatically reduced activity with the variant of Phe to Ala or Lys at the P2 position.

The side chain of P3-Leu was oriented to the bulk solvent region. The backbone of Leu interacted with Gly164 of the protease via two hydrogen bonds. The P4-Ala residue was a relatively con-

served residue in the natural joint sequences (Table 1). Two backbone hydrogen bonds were formed between Ala and the main-chain groups of Asn126 and Ser128, respectively. The size and hydrophobic characters of a hydrophobic pocket of the S4 subsite well accommodated the methyl group of Ala. Substrate P12, which contained an Ala-to-Leu mutation at the P4 position, represented moderate cleavage potency, but P16, containing an Ala-to-Phe mutation, showed weak cleavage efficiency, indicating that the S4 pocket is tolerant to a relatively small residue. There were no apparent pockets and interactions in the protease for the P5 and P6 residues of the substrate. P5 Glu contacted with the protease only by a hydrogen bond formed with the backbone of Asn126 (Fig. 4D). With a Glu-to-Ala mutation, P11 showed a 5-fold reduction of cleavage efficiency. We speculated that this accounts for the location of the P5 position at the entry of the substrate-binding site.

Z' factor analysis. In order to assess the quality of this fluorogenic model substrate-based assay for the screening of EV71 3C protease inhibitors, the value of the Z' factor was determined. A Z' factor of >0.5 means a robust and reliable indicator for high-throughput screening assay (32). A scatter plot of fluorescence units is shown in Fig. 5, which shows the assay range and data derivation for the positive control (substrate fluorescence after incubation with EV71 3C protease) and negative control (background of the substrate). The Z' factor was obtained from 60

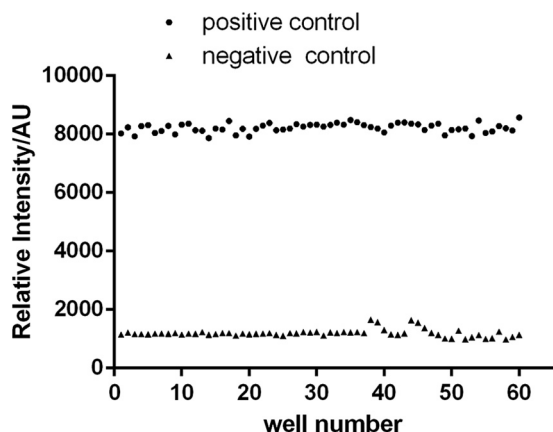


FIG 5 Validation of the quality of the EV71 3C protease assay. The assay was performed using 20 μ M substrate P08 [NMA-IEALFQGPPK(DNP)FR] with 1 μ M protease (positive control) ($n = 60$, circles) and without protease (negative control) ($n = 60$, triangles). Experiments were repeated more than three times with consistent results.

independent positive controls containing 20 μ M P08 [NMA-IEALFQGPPK(DNP)FR] and 1 μ M protease and negative controls containing 20 μ M P08 without protease. The Z' factor was determined as 0.87 ± 0.05 , which indicates a good overall quality of the assay and the required robustness for further high-throughput screening application.

Evaluation of inhibitors. To validate the application of the established fluorogenic substrates for EV71 3C protease inhibitor screening, two published compounds (compounds 1 and 2) and one novel compound (compound 3) were synthesized to evaluate their inhibitory activities against EV71 3C protease. The inhibitory activity of each compound was examined using peptide P08 as the substrate. Cleavage of the substrate by EV71 3C protease in the presence of various concentrations of the inhibitor was mon-

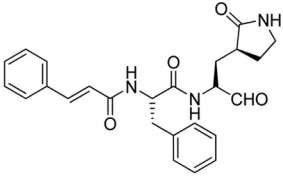
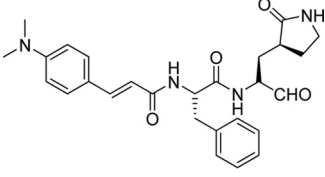
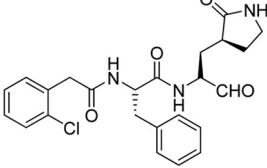
itored with a 96-well fluorescence plate reader, as described above. Aldehyde 1, which was previously reported to inhibit EV71 protease (26), showed efficacy with an IC_{50} of $4.97 \pm 0.28 \mu$ M in this study. With a dimethylamine substitution at the benzene group of the cinnamoyl fragment, derivative 2 demonstrated a small increase of anti-EV71 activity ($IC_{50} = 3.66 \pm 0.43 \mu$ M), which is consistent with the previous report (26). As shown in Table 3, we synthesized a novel compound (compound 3) with a 2-chloride-phenylacetyl substitution instead of the cinnamoyl of compound 1. The biological analysis revealed that the efficacy of compound 3 ($IC_{50} = 1.89 \pm 0.25 \mu$ M) is twice that reported for compounds 1 and 2.

We next determined the inhibitory activities of the tested compounds after treatment with EV71(FY)-Luc pseudotype virus-infected RD cells. Consistently, the results indicated that the virus proliferation was also significantly attenuated by the treatment with the three compounds, with EC_{50} s of 3.38 ± 0.47 , 3.07 ± 0.56 , and $4.54 \pm 0.51 \mu$ M for tested compounds 1, 2, and 3, respectively. The results of the cytotoxicity assay revealed that up to 100 μ M, all three compounds had no cytotoxic effect on the viability of RD cells.

DISCUSSION

EV71 encodes a polyprotein in a single open reading frame, where the polyprotein is processed by 3C protease and 2A protease into individual functional proteins. Thus, 3C protease serves as an excellent target for developing inhibitors against EV71. In previous studies, together with the research on EV71 protease structure, a number of substrates were investigated by HPLC assay, and two fluorogenic peptides, P01 (DabcyI-RTATVQGPSLDFKE-Edans) and P02 (DabcyI-TSAVLQSGFRKME-Edans), were also used to study inhibitor activity (23, 25, 26). In this study, we report the substrate specificities and complete kinetic parameters of the EV71 3C protease for a small set of synthesized fluorogenic pep-

TABLE 3 Peptidomimetic inhibitors against EV71 3C protease^a

Compound no.	Structure	IC_{50} (μ M)	EC_{50} (μ M)	CC_{50} (μ M)
1		4.97 ± 0.28	3.38 ± 0.47	>100
2		3.66 ± 0.43	3.07 ± 0.56	>100
3		1.89 ± 0.25	4.54 ± 0.51	>100

^a Data are means and standard deviations from triplicate experiments.

tide substrates. We have established a robust fluorogenic substrate model for the screening of EV71 protease inhibitors.

In analogy to a number of specificity studies on the viral proteases (26, 39–43), we assayed the control fluorogenic peptide substrates P01 and P02 and 15 novel peptide substrates based on the cleavage sites of EV71 polyprotein. The substrates P01 and P02 exhibited inconsistent cleavage efficiency in the previous studies (23, 26). Our data suggested that the substrate P02 and its analogue P04 [NMA-TSAVLQSGFRK(DNP)M] could be cleavable but with a lower relatively enzymatic activity (Fig. 2A). The binding affinity and cleavage efficiency for P01 were higher than those for P02 for EV71 3C protease, and this result is consistent with the report by Cui et al. (23). More importantly, the novel peptide substrate P08 [NMA-IEALFQGPPK(DNP)FR], derived from the 2C-3A junction of the EV71 polyprotein, was determined to be the most efficient substrate among all tested peptides. It represented an approximately 8-fold-higher k_{cat}/K_m than that for the control substrate P01 (Fig. 2B), indicating effective and fast separation of the P3 region from the P2 region of the viral polyprotein. Supportive evidence comes from the report by Lu et al. (25), who demonstrated that the peptide IGNTIEALFQGPPKFR, corresponding to 2C-3A junction site of CVA16, was most efficiently processed by CVA16 protease via the HPLC assay ($V = 8.37 \pm 1.93 \mu\text{M}/\text{min}$). It is also noteworthy that a single variant of the P1'-P5 residues within the peptide P08 could lead to a decrease in cleavage efficiency. When the relatively large hydrophobic amino acid Phe at P2 position was replaced by the relatively small hydrophobic amino acid Ala or the basic amino acid Lys, P14 or P17 showed a very low cleavage rate, for which the precise kinetic parameters K_m and k_{cat} cannot be determined. Despite the fact that Ser also exists in the natural cleavage sites, replacement of Gly at the P1' position of P08 by Ser led to dramatic decrease in the cleavage efficiency. The variant study revealed that the P2 and P1' residues would allow the substrate P08 to bind more tightly to EV71 protease.

Based on the enzymatic assay, we noted that the same peptide with different fluorescence-quenching groups (P01 versus P03, P02 versus P04, and P08 versus P10) showed different cleavage efficiencies. The most efficient substrate, P08, and its analogue P10, with the same peptide sequence but different FRET pairs, showed significantly different kinetic constants k_{cat}/K_m of 11.8 ± 0.82 and $2.69 \pm 0.15 \text{ mM}^{-1} \text{ min}^{-1}$, respectively. We suspected that the N-terminal group or C-terminal fluorescent/quencher groups favorably interact with EV71 3C protease via van der Waals interactions. Further experiments are needed to confirm this hypothesis.

Molecular dynamics simulations were done to study the substrate-enzyme interactions. Similar to the previously determined binding mode in the substrate FAGLRQAVTQGFPTL complexed with CVA16 protease (25), the P6 to P1' portions of substrates bind to the active site of EV71 3C protease. We observed that a conserved residue Arg39 provided a striking rotation toward to the substrate in the MD model of substrate P08 and EV71 3C protease. This rotation afforded an increased interaction (3.4 \AA) between Arg39 and Phe at the P2 position of P08. In contrast, Arg39 still maintained the original conformation in other MD modes of substrates without Phe at the P2 position. We believe that Arg39 may assist the process of cleavage of the substrate by the EV71 3C protease.

Finally, two reported compounds as references (compounds 1 and 2) and a novel compound (compound 3) were synthesized to

validate the assay for the screening of EV71 protease inhibitors. In addition to the two reference compounds, the novel compound 3 was found to inhibit EV71 3C protease, with an IC_{50} of $1.89 \pm 0.25 \mu\text{M}$. Moreover, the inhibitor suppressed the proliferation of EV71 in RD cells without cytotoxicity at the highest tested concentration ($\text{EC}_{50} = 4.54 \pm 0.51 \mu\text{M}$, $\text{CC}_{50} > 100 \mu\text{M}$), indicating that it could be a leading compound for anti-EV71 drug discovery.

In conclusion, we describe a systematic biological characterization of EV71 3C protease with fluorogenic peptide substrates. A fluorogenic peptide, P08 [NMA-IEALFQGPPK(DNP)FR], with a high substrate specificity constant (k_{cat}/K_m of $11.8 \pm 0.82 \text{ mM}^{-1} \text{ min}^{-1}$) and which undergoes considerable proteolysis in the presence of EV71 3C protease was identified. P08 is an ideal substrate for biochemical characterization of EV71 3C protease. A high-quality screening assay of EV71 3C protease inhibitors with a high Z' factor (0.87 ± 0.05) was established. A novel compound (compound 3) ($\text{IC}_{50} = 1.89 \pm 0.25 \mu\text{M}$) that effectively suppressed the proliferation of EV71 (strain Fuyang) in RD cells with a highly selective index ($\text{EC}_{50} = 4.54 \pm 0.51 \mu\text{M}$, $\text{CC}_{50} > 100 \mu\text{M}$) was discovered using this assay. The biochemical assay was further validated by the determination of low IC_{50} s of three synthesized EV71 3C protease inhibitors.

ACKNOWLEDGMENTS

This work was supported by the National Natural Science Foundation of China (grant no. 21202087 and 81102374), the National Basic Research Program of China (973 program, grant no. 2013CB911104), the Fundamental Research Funds for the Central Universities (grant no. 65124002), the Tianjin Science and Technology Program (grant no. 13JCYBJC24300 and 13JCQNJC13100), the Specialized Research Fund for the Doctoral Program of Higher Education Ministry of Education of China (grant no. 2120031120049), and the "111" Project of the Ministry of Education of China (project no. B06005).

REFERENCES

1. Chan KP, Goh KT, Chong CY, Teo ES, Lau G, Ling AE. 2003. Epidemic hand, foot and mouth disease caused by human enterovirus 71, Singapore. *Emerg Infect Dis* 9:78–85. <http://dx.doi.org/10.3201/eid1301.020112>.
2. Yang Y, Wang H, Gong E, Du J, Zhao X, McNutt MA, Wang S, Zhong Y, Gao Z, Zheng J. 2009. Neuropathology in 2 cases of fatal enterovirus type 71 infection from a recent epidemic in the People's Republic of China: a histopathologic, immunohistochemical, and reverse transcription polymerase chain reaction study. *Hum Pathol* 40:1288–1295. <http://dx.doi.org/10.1016/j.humpath.2009.01.015>.
3. Chen S-C, Chang H-L, Yan T-R, Cheng Y-T, Chen K-T. 2007. An eight-year study of epidemiologic features of enterovirus 71 infection in Taiwan. *Am J Trop Med Hyg* 77:188–191.
4. Chua K, Chua B, Lee C, Chem Y, Ismail N, Kiyu A, Kumarasamy V. 2007. Genetic diversity of enterovirus 71 isolated from cases of hand, foot and mouth disease in the 1997, 2000 and 2005 outbreaks, Peninsular Malaysia. *Malays J Pathol* 29:69–78.
5. Chen C, Wang Y, Shan C, Sun Y, Xu P, Zhou H, Yang C, Shi P-Y, Rao Z, Zhang B. 2013. Crystal structure of enterovirus 71 RNA-dependent RNA polymerase complexed with its protein primer VPg: implication for a trans mechanism of VPg uridylylation. *J Virol* 87:5755–5768. <http://dx.doi.org/10.1128/JVI.02733-12>.
6. Ming Z, Wang W, Xie Y, Ding P, Chen Y, Jin D, Sun Y, Xia B, Yan L, Lou Z. 2014. Crystal structure of the novel di-nucleotide cyclase from *Vibrio cholerae* (DncV) responsible for synthesizing a hybrid cyclic GMP-AMP. *Cell Res* 24:1270–1273. <http://dx.doi.org/10.1038/cr.2014.123>.
7. Sun Y, Guo Y, Lou Z. 2014. Formation and working mechanism of the picornavirus VPg uridylylation complex. *Curr Opin Virol* 9:24–30. <http://dx.doi.org/10.1016/j.coviro.2014.09.003>.
8. Gong P, Kortus MG, Nix JC, Davis RE, Peersen OB. 2013. Structures of coxsackievirus, rhinovirus, and poliovirus polymerase elongation complexes solved by engineering RNA mediated crystal contacts. *PLoS One* 8:e60272. <http://dx.doi.org/10.1371/journal.pone.0060272>.

9. McMinn PC. 2002. An overview of the evolution of enterovirus 71 and its clinical and public health significance. *FEMS Microbiol Rev* 26:91–107. <http://dx.doi.org/10.1111/j.1574-6976.2002.tb00601.x>.
10. Wu Y, Lou Z, Miao Y, Yu Y, Dong H, Peng W, Bartlam M, Li X, Rao Z. 2010. Structures of EV71 RNA-dependent RNA polymerase in complex with substrate and analogue provide a drug target against the hand-foot-and-mouth disease pandemic in China. *Protein Cell* 1:491–500. <http://dx.doi.org/10.1007/s13238-010-0061-7>.
11. Qing J, Wang Y, Sun Y, Huang J, Yan W, Wang J, Su D, Ni C, Li J, Rao Z. 2014. Cyclophilin A associates with enterovirus-71 virus capsid and plays an essential role in viral infection as an uncoating regulator. *PLoS Pathol* 10:e1004422. <http://dx.doi.org/10.1371/journal.ppat.1004422>.
12. Hwang Y-C, Chen W, Yates MV. 2006. Use of fluorescence resonance energy transfer for rapid detection of enteroviral infection in vivo. *Appl Environ Microbiol* 72:3710–3715. <http://dx.doi.org/10.1128/AEM.72.5.3710-3715.2006>.
13. Bishop NE, Anderson DA. 1993. RNA-dependent cleavage of VP0 capsid protein in provirions of hepatitis A virus. *Virology* 197:616–623. <http://dx.doi.org/10.1006/viro.1993.1636>.
14. Marcotte LL, Wass AB, Gohara DW, Pathak HB, Arnold JJ, Filman DJ, Cameron CE, Hogle JM. 2007. Crystal structure of poliovirus 3CD protein: virally encoded protease and precursor to the RNA-dependent RNA polymerase. *J Virol* 81:3583–3596. <http://dx.doi.org/10.1128/JVI.02306-06>.
15. Matthews DA, Smith WW, Ferre RA, Condon B, Budahazi G, Sllson W, Villafranca J, Janson CA, McElroy H, Gribkov C. 1994. Structure of human rhinovirus 3C protease reveals a trypsin-like polypeptide fold, RNA-binding site, and means for cleaving precursor polypeptide. *Cell* 77:761–771. [http://dx.doi.org/10.1016/0092-8674\(94\)90059-0](http://dx.doi.org/10.1016/0092-8674(94)90059-0).
16. Sun Y, Wang Y, Shan C, Chen C, Xu P, Song M, Zhou H, Yang C, Xu W, Shi P-Y. 2012. Enterovirus 71 VPg uridylation uses a two-molecular mechanism of 3D polymerase. *J Virol* 86:13662–13671. <http://dx.doi.org/10.1128/JVI.01712-12>.
17. Weng K-F, Li M-L, Hung C-T, Shih S-R. 2009. Enterovirus 71 3C protease cleaves a novel target CstF-64 and inhibits cellular polyadenylation. *PLoS Pathol* 5:e1000593. <http://dx.doi.org/10.1371/journal.ppat.1000593>.
18. Clark ME, Hämmerle T, Wimmer E, Dasgupta A. 1991. Poliovirus proteinase 3C converts an active form of transcription factor IIIC to an inactive form: a mechanism for inhibition of host cell polymerase III transcription by poliovirus. *EMBO J* 10:2941.
19. Falk M, Grigera P, Bergmann I, Zibert A, Multhaup G, Beck E. 1990. Foot-and-mouth disease virus protease 3C induces specific proteolytic cleavage of host cell histone H3. *J Virol* 64:748–756.
20. Weidman MK, Yalamanchili P, Ng B, Tsai W, Dasgupta A. 2001. Poliovirus 3C protease-mediated degradation of transcriptional activator p53 requires a cellular activity. *Virology* 291:260–271. <http://dx.doi.org/10.1006/viro.2001.1215>.
21. Yalamanchili P, Datta U, Dasgupta A. 1997. Inhibition of host cell transcription by poliovirus: cleavage of transcription factor CREB by poliovirus-encoded protease 3Cpro. *J Virol* 71:1220–1226.
22. Shang L, Xu M, Yin Z. 2013. Antiviral drug discovery for the treatment of enterovirus 71 infections. *Antiviral Res* 97:183–194. <http://dx.doi.org/10.1016/j.antiviral.2012.12.005>.
23. Cui S, Wang J, Fan T, Qin B, Guo L, Lei X, Wang J, Wang M, Jin Q. 2011. Crystal structure of human enterovirus 71 3C protease. *J Mol Biol* 408:449–461. <http://dx.doi.org/10.1016/j.jmb.2011.03.007>.
24. Wang J, Fan T, Yao X, Wu Z, Guo L, Lei X, Wang J, Wang M, Jin Q, Cui S. 2011. Crystal structures of enterovirus 71 3C protease complexed with rupintrivir reveal the roles of catalytically important residues. *J Virol* 85:10021–10030. <http://dx.doi.org/10.1128/JVI.05107-11>.
25. Lu G, Qi J, Chen Z, Xu X, Gao F, Lin D, Qian W, Liu H, Jiang H, Yan J. 2011. Enterovirus 71 and coxsackievirus A16 3C proteases: binding to rupintrivir and their substrates and anti-hand, foot, and mouth disease virus drug design. *J Virol* 85:10319–10331. <http://dx.doi.org/10.1128/JVI.00787-11>.
26. Kuo C-J, Shie J-J, Fang J-M, Yen G-R, Hsu JT-A, Liu H-G, Tseng S-N, Chang S-C, Lee C-Y, Shih S-R. 2008. Design, synthesis, and evaluation of 3C protease inhibitors as anti-enterovirus 71 agents. *Bioorg Med Chem* 16:7388–7398. <http://dx.doi.org/10.1016/j.bmc.2008.06.015>.
27. Haugland RP, Yguerabide J, Stryer L. 1969. Dependence of the kinetics of singlet-singlet energy transfer on spectral overlap. *Proc Natl Acad Sci U S A* 63:23–30. <http://dx.doi.org/10.1073/pnas.63.1.23>.
28. Li B, Wang Q, Pan X, de Castro IF, Sun Y, Guo Y, Tao X, Risco C, Sui S-F, Lou Z. 2013. Bunyamwera virus possesses a distinct nucleocapsid protein to facilitate genome encapsidation. *Proc Natl Acad Sci U S A* 110:9048–9053. <http://dx.doi.org/10.1073/pnas.1222552110>.
29. Wu C, Cai Q, Chen C, Li N, Peng X, Cai Y, Yin K, Chen X, Wang X, Zhang R. 2013. Structures of enterovirus 71 3C proteinase (strain E2004104-TW-CDC) and its complex with rupintrivir. *Acta Crystallogr Sect D Biol Crystallogr* 69:866–871. <http://dx.doi.org/10.1107/S0907444913002862>.
30. Guo Y, Wang W, Ji W, Deng M, Sun Y, Zhou H, Yang C, Deng F, Wang H, Hu Z. 2012. Crimean-Congo hemorrhagic fever virus nucleoprotein reveals endonuclease activity in bunyaviruses. *Proc Natl Acad Sci U S A* 109:5046–5051. <http://dx.doi.org/10.1073/pnas.1200808109>.
31. Hirata IY, Cezari MHS, Nakaie CR, Boschov P, Ito AS, Juliano MA, Juliano L. 1995. Internally quenched fluorogenic protease substrates: solid-phase synthesis and fluorescence spectroscopy of peptides containing ortho-aminobenzoyl/dinitrophenyl groups as donor-acceptor pairs. *Lett Pept Sci* 1:299–308. <http://dx.doi.org/10.1007/BF00119771>.
32. Zhang J-H, Chung TD, Oldenburg KR. 1999. A simple statistical parameter for use in evaluation and validation of high throughput screening assays. *J Biomol Screen* 4:67–73. <http://dx.doi.org/10.1177/108705719900400206>.
33. Klauda JB, Brooks BR. 2008. CHARMM force field parameters for nitroalkanes and nitroarenes. *J Chem Theor Comput* 4:107–115. <http://dx.doi.org/10.1021/ct700191v>.
34. Roche O, Kiyama R, Brooks CL. 2001. Ligand-protein database: linking protein-ligand complex structures to binding data. *J Med Chem* 44:3592–3598. <http://dx.doi.org/10.1021/jm000467k>.
35. Jorgensen WL, Chandrasekhar J, Madura JD, Impey RW, Klein ML. 1983. Comparison of simple potential functions for simulating liquid water. *J Chem Phys* 79:926–935. <http://dx.doi.org/10.1063/1.445869>.
36. Pastor RW, Brooks BR, Szabo A. 1988. An analysis of the accuracy of Langevin and molecular dynamics algorithms. *Mol Phys* 65:1409–1419. <http://dx.doi.org/10.1080/00268978800101881>.
37. Shang L, Wang Y, Qing J, Shu B, Cao L, Lou Z, Gong P, Sun Y, Yin Z. 2014. An adenosine nucleoside analogue NS2B-NS3 inhibits EV71 proliferation. *Antiviral Res* 112:47–58. <http://dx.doi.org/10.1016/j.antiviral.2014.10.009>.
38. Zhang L, Lawson HL, Harish VC, Huff JD, Knovich MA, Owen J. 2006. Creation of a recombinant peptide substrate for fluorescence resonance energy transfer-based protease assays. *Anal Biochem* 358:298–300. <http://dx.doi.org/10.1016/j.ab.2006.06.022>.
39. Gouvea I, Izidoro M, Judice W, Cezari M, Caliendo G, Santagada V, Dos Santos C, Queiroz M, Juliano M, Young P. 2007. Substrate specificity of recombinant dengue 2 virus NS2B-NS3 protease: influence of natural and unnatural basic amino acids on hydrolysis of synthetic fluorescent substrates. *Arch Biochem Biophys* 457:187–196. <http://dx.doi.org/10.1016/j.abb.2006.11.005>.
40. Lou Z, Sun Y, Rao Z. 2014. Current progress in antiviral strategies. *Trends Pharmacol Sci* 35:86–102. <http://dx.doi.org/10.1016/j.tips.2013.11.006>.
41. Shiryaev SA, Ratnikov BI, Aleshin AE, Kozlov IA, Nelson NA, Lebl M, Smith JW, Liddington RC, Strongin AY. 2007. Switching the substrate specificity of the two-component NS2B-NS3 flavivirus proteinase by structure-based mutagenesis. *J Virol* 81:4501–4509. <http://dx.doi.org/10.1128/JVI.02719-06>.
42. Tsai M-T, Cheng Y-H, Liu Y-N, Liao N-C, Lu W-W, Kung S-H. 2009. Real-time monitoring of human enterovirus (HEV)-infected cells and anti-HEV 3C protease potency by fluorescence resonance energy transfer. *Antimicrob Agents Chemother* 53:748–755. <http://dx.doi.org/10.1128/AAC.00841-08>.
43. Zhou H, Sun Y, Guo Y, Lou Z. 2013. Structural perspective on the formation of ribonucleoprotein complex in negative-sense single-stranded RNA viruses. *Trends Microbiol* 21:475–484. <http://dx.doi.org/10.1016/j.tim.2013.07.006>.
44. Ryckaert J-P, Ciccotti G, Berendsen HJC. 1977. Numerical integration of the Cartesian equations of motion of a system with constraints: molecular dynamics of *n*-alkanes. *J Comput Phys* 23:327–341. [http://dx.doi.org/10.1016/0021-9991\(77\)90098-5](http://dx.doi.org/10.1016/0021-9991(77)90098-5).